Full Articles

Chemical bond inside endohedral complexes $H@C_{59}B$ and $H@C_{59}P$

A. L. Buchachenko,[a,b] and N. N. Breslavskaya[b]★

[a]Institute of Problems of Chemical Physics, Russian Academy of Sciences,
1 prosp. Akad. Semenova, 142432 Chernogolovka, Moscow Region, Russian Federation.
Fax: +7 (495) 938 2484. E-mail: spinchem@chph.ras.ru
[b]N. S. Kurnakov Institute of General and Inorganic Chemistry, Russian Academy of Sciences,
31 Leninsky prosp., 119991 Moscow, Russian Federation.
Fax: +7 (495) 954 1279. E-mail: breslav@igic.ras.ru

The geometries, electronic structures, and spin densities on the atoms of paramagnetic heterofullerenes $C_{59}X$ (X = B, P) and their endohedral derivatives $H@C_{59}X$ were obtained from B3LYP/6-31G* density functional calculations. The encapsulated hydrogen atom can form a C—H bond inside the fullerene sphere. The energies of the C—H(*endo*) bonds are 40—50 kcal mol^{-1} lower than those of the corresponding *exo*-bonds.

Key words: heterofullerenes, quantum chemical calculations, density functional theory, spin density, hyperfine coupling constant, binding energy.

Endohedral complexes $H@C_{59}X$ of paramagnetic heterofullerenes $C_{59}X$ (X = B, N, P)[1—4] have not been reported so far. They can be obtained similarly to the complexes $H@C_{60}$ or $T@C_{60}$;[5] however, there is little sense in doing such a labor-consuming work, although the syntheses of the endohedral complexes $K@C_{59}B$ and $K@C_{58}B_2$ have been documented.[4] The aim of this work was to calculate the energy states of systems under study in the case where an H atom moves from the center of the fullerene sphere toward different atoms of $C_{59}X$ fullerene, *i.e.*, to assess the possibility of formation of the *endo*-bond between the encapsulated hydrogen atom and the $C_{59}X$ heterofullerene that form the endohedral complex. Earlier,[6] this problem was solved for $H@C_{59}N$. Here, this was done for $H@C_{59}B$ and $H@C_{59}P$ and the results obtained are generalized for all the three systems.

Calculation Procedure

Geometric parameters of the systems $C_{59}X$ (doublet spin state) and $H@C_{59}X$ (in the singlet and triplet states) were optimized in the framework of the density functional theory (DFT) with the B3LYP three-parameter exchange-correlation functional and the 6-31G* basis set[7] using the GAUSSIAN-98 program.[8] This approximation provides a quite accurate and reliable description of the structure and properties of related systems.[6,9] The method was also used to calculate the isotropic hyperfine coupling (HFC) constants $a(X)$ and $a(^{13}C)$ for the optimized structures of the $C_{59}X$ systems and to perform vibra-

Published in Russian in *Izvestiya Akademii Nauk. Seriya Khimicheskaya,* No. 7, pp. 1239—1243, July, 2007.
1066-5285/07/5607-1283

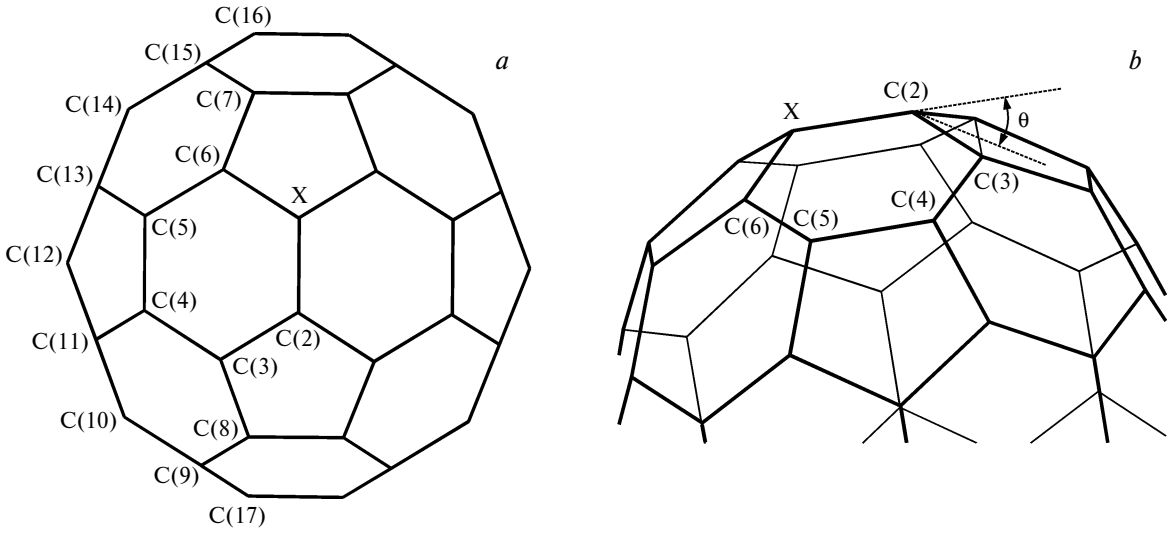

Fig. 1. Schematic view of $C_{59}X^{\bullet}$ radicals (X = N, P, B) (*a*) and position of the C(2) atom determined by the angle θ (*b*).

tional frequency analysis for the endohedral derivatives of H—C_{59}X in which the H atom forms a chemical bond with a carbon atom. Based on the results of the vibrational frequency analysis, the optimized structures were characterized as corresponding to energy minima on the potential energy surfaces.

Results and Discussion

Geometric parameters. Geometric parameters and electronic properties of the $C_{59}X$ systems (Fig. 1) were repeatedly studied by theoretical[1,6,10—13] and experimental[1—4,12] methods. The calculated bond lengths seem to be quite reliable, namely, the 6/6- and 6/5-bond lengths in the C_{60} molecule are 1.392 and 1.452 Å, respectively (*cf.* 1.395 and 1.453 Å obtained from B3LYP/6-31G** calculations[14] and the experimental values[15] equal to 1.388(9) and 1.432(5) Å).

The calculated bond lengths in the $C_{59}X$ systems (Table 1) are similar to those calculated by other methods for $C_{59}B$,[10] $C_{59}N$,[1,10—12] and $C_{59}P$.[13] The C—X bonds and adjacent C—C bonds are longer than corresponding conventional bonds due to strain in the polyhedral cage fragment near the X atom. The optimized C(2)—X bond length is 1.526 (X = B), 1.408 (X = N), and 1.809 Å (X = P); hereafter, we will discuss all the three endofullerenes with X = B, N, and P to point some regularities in their structural and chemical properties.

In $C_{59}P$, the fullerene cage near the heteroatom is much more strained compared to $C_{59}N$ and $C_{59}B$. The θ angle determining the position of the C(2) atom (see Fig. 1, *b*) is 35.6 ($C_{59}B$), 30.5 ($C_{59}N$), and 22° ($C_{59}P$). Thus, the smaller the X atom the weaker the cage distortion.

The formation of H@$C_{59}X$ endofullerenes leaves the $C_{59}X$ cage structure almost undistorted. Namely, the bond lengths change insignificantly and the θ angle decreases by 2° for H@$C_{59}B$ and by 6—7° for H@$C_{59}N$ and H@$C_{59}P$. The key geometric parameters of the $C_{59}X$ and H@$C_{59}X$ species are listed in Table 1.

Atomic charges and spin density. The calculated Mulliken atomic charges of carbons in the compounds $C_{59}X$ are small (from −0.05 to 0.01 for $C_{59}B$, from −0.01 to 0.21 for $C_{59}N$, and from −0.20 to 0.05 for $C_{59}P$), whereas the charges on the heteroatoms are 0.14 (X = B), −0.61 (X = N), and 0.49 (X = P). Partial charge transfer from neighboring carbon atoms to the N atom oc-

Table 1. Geometric parameters of compounds $C_{59}X$ (doublet state) and H@$C_{59}X$ (singlet state)

Compound	Bond length/Å				Angle/deg			
	C(2)—X	C(6)—X	C(2)—C(3)	C(2)—H	C(3)—C(2)—C(3)	C(3)—C(2)—X	C(6)—X—C(2)	θ
$C_{59}N$	1.408	1.424	1.434	—	108.7	120.1	118.9	30.5
H@$C_{59}N$	1.384	1.422	1.432	3.507	109.8	121.7	118.3	23.9
$C_{59}P$	1.809	1.840	1.436	—	108.8	122.7	97.3	22.0
H@$C_{59}P$	1.796	1.829	1.428	3.625	110.2	123.2	96.9	16.7
$C_{59}B$	1.526	1.548	1.443	—	107.7	118.7	118.6	35.6
H@$C_{59}B$	1.526	1.548	1.442	3.624	107.7	118.7	118.6	33.3

curs; contrary to this, the P and B atoms act as charge donors.

Unlike unsubstituted C_{60} fullerene with I_h symmetry, the $C_{59}X$ molecules having C_s symmetry are polar; the calculated dipole moments are 0.1, 1.2, and 0.6 D for X = B, N, and P, respectively.

The spin density distribution in the $C_{59}X$ radicals is shown in Fig. 2. The highest positive spin density is localized on the C(2) atom. The spin density is distributed over the system of π-bonds in such a manner that all the even carbon atoms bear positive spin density, which gradually decreases with the distance from the C(2) atom to the C(8) atom. Then, it slightly increases on the C(10) atom and again decreases almost to zero on the C(14) atom and more distant atoms.

The spin density on all the odd carbon atoms is negative, being largest in absolute value on the C(3) atom. Then, it decreases almost to zero on the C(5) and C(7) atoms, increases (in absolute value) on the C(9) and C(11) atoms, and again decreases almost to zero on more distant atoms. Thus, all the $C_{59}X$ radicals show a common pattern of the spin density distribution over the atoms of the fullerene sphere. Namely, the positive spin density is mainly distributed over orbitals of the even carbon atoms by the spin delocalization mechanism, whereas spin delocalization over the odd carbon atoms mainly occurs by the spin polarization mechanism involving creation of negative spin density on these atoms. Both positive and negative spin density decreases with the distance from the C(2) atom. This situation is typical of organic radicals.[16]

The X atoms bear positive spin density (see Fig. 2), which is, however, lower than for the C(2) atom. It follows that the spin density is transferred to the X orbitals by both mechanisms (spin delocalization and spin polarization) with partial compensation, the former making the major contribution.

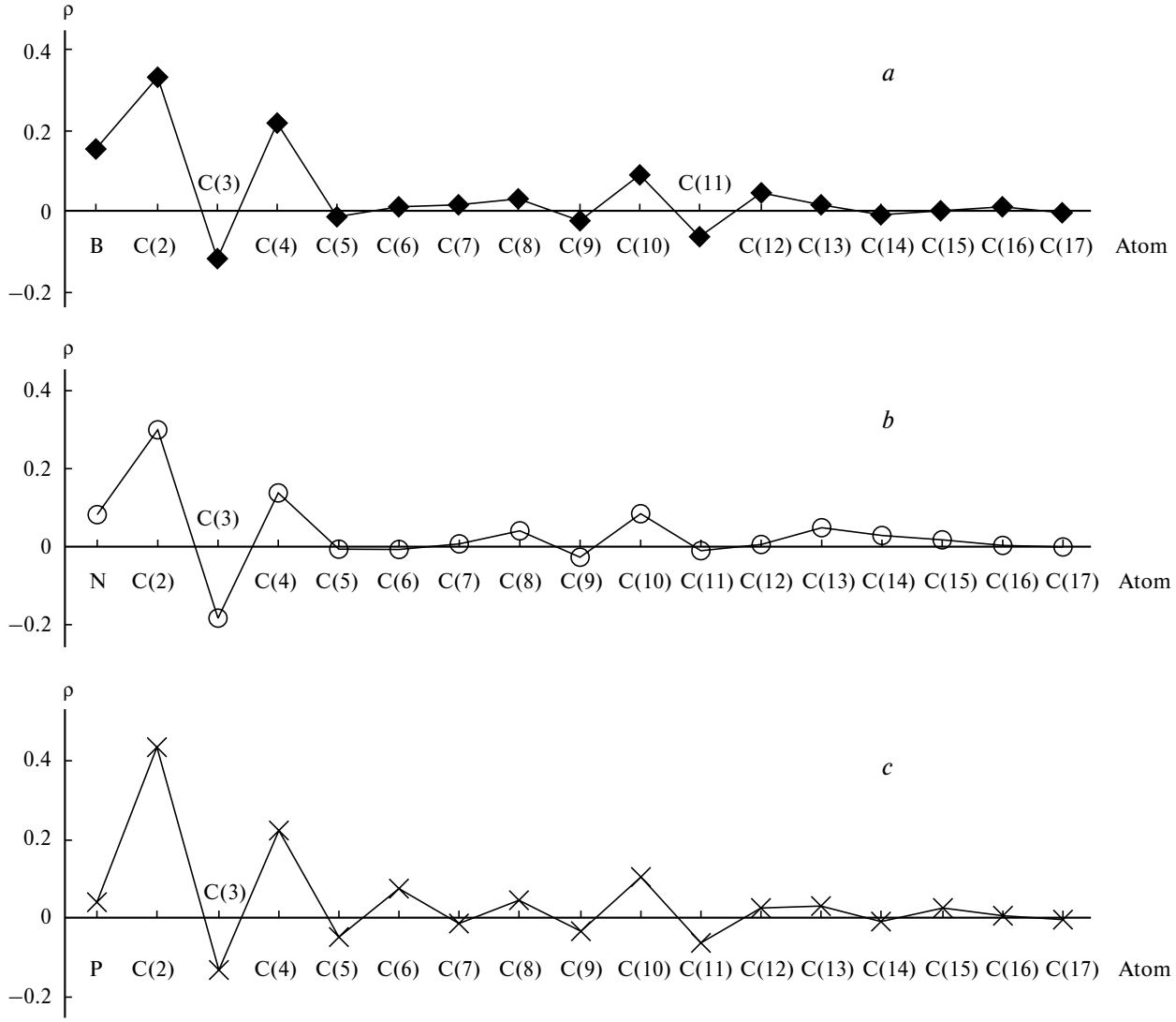

Fig. 2. Spin density distribution over atoms of $C_{59}X$ radicals: X = B (*a*), N (*b*), and P (*c*).

Table 2. HFC constants (a) on the X and ^{13}C atoms in $C_{59}X$ systems

Atom X	a/T			
	X	C(2)	C(3)	C(4)
B	0.25	1.41	−0.82	1.06
N*	0.41	1.79	−0.65	0.68
	(0.36)	(1.18)	(−0.52)	(0.48)
P	10.18	2.70	−0.98	1.16

* Experimental values[12] are given in parentheses.

Table 2 lists the HFC constants a calculated for the $C_{59}X$ molecules. The calculated and experimental[12] a values for $C_{59}N$ are in reasonable agreement.

Energy characteristics. We calculated the structures of the H—$C_{59}X$ systems in the singlet and triplet states. All the singlet structures are energetically more favorable than the corresponding triplet species; therefore, only the singlet structures will be considered below.

Reaction trajectories. The potential energy profiles were calculated by varying the distance between the center of the $C_{59}X$ sphere and the H atom moving along the radius from the center to the X, C(2), C(3), C(4), *etc.*, atoms at the same (namely, optimized) bond lengths and bond angles in the $C_{59}X$ systems. The distance R between the center of the $C_{59}X$ sphere and the H atom was varied in the range 0 Å $\leq R \leq$ 6.0 Å. The profiles of the motion of the H atom from the center to the C(2) atom bearing the maximum unpaired electron density are shown in Fig. 3 and can be divided into two groups characterizing the motion of the H atom along "internal" H—C(2) trajectories from the center of the fullerene sphere and the motion of a distant H atom from the outside of the sphere to the C(2) atom. Figure 3 shows that for all the three $C_{59}X$ radicals the former group of the energy profiles exhibit minima lying below the energy of the H@$C_{59}X$ system and corresponding to the formation of a C(2)—H bond inside the fullerene sphere (*endo*-H—C(2) bond).

The "external" trajectories correspond to attraction (see Fig. 3). The strongest bonding was obtained for the

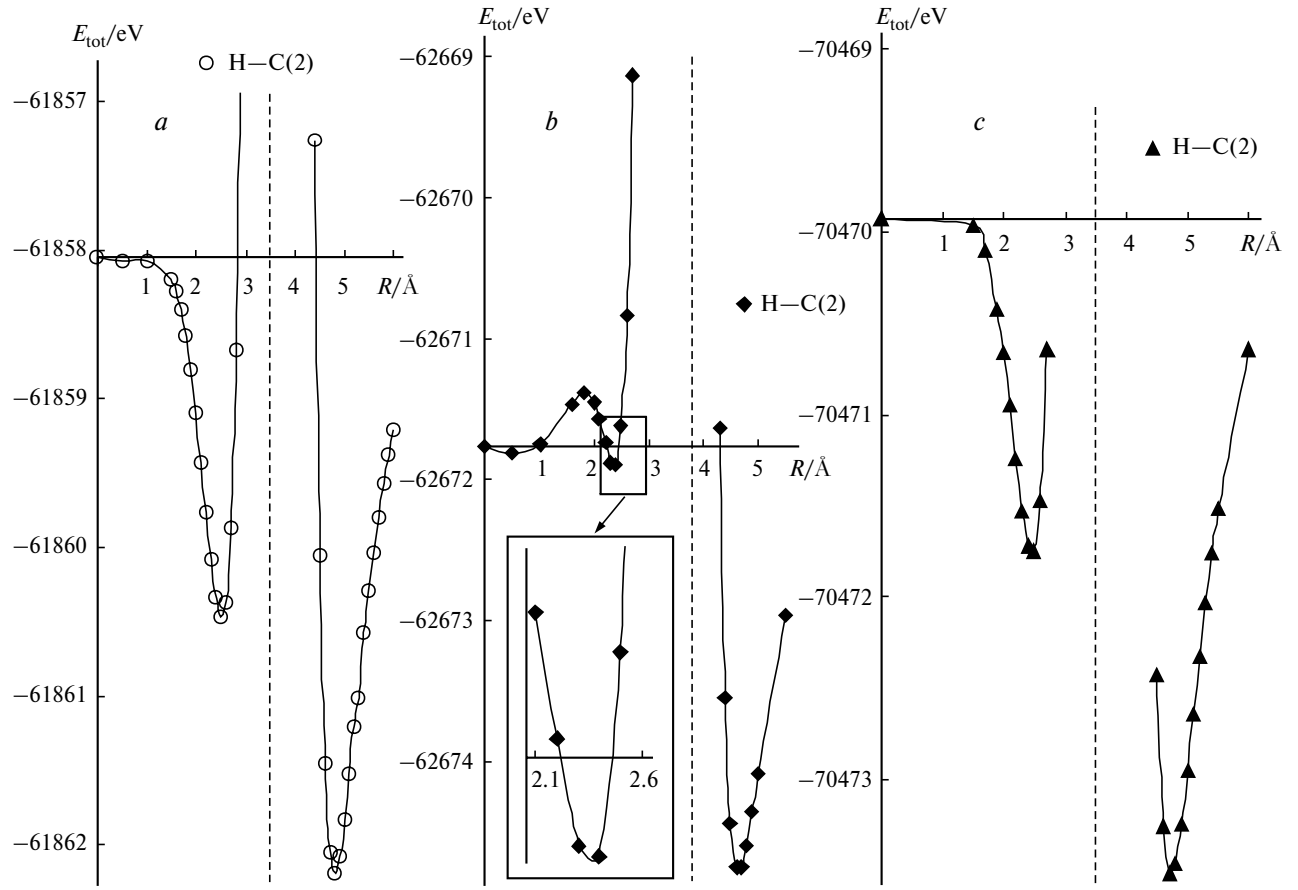

Fig. 3. Potential energy profiles along the H—C(2) trajectory for the systems H + $C_{59}B$ (*a*), H + $C_{59}N$ (*b*), and H + $C_{59}P$ (*c*). At $R = 0$, the atom H is located at the center of the $C_{59}X$ sphere; the dashed vertical line at $R = 3.5$ Å corresponds to position of the atoms of the fullerene cage; the range 0 Å $\leq R \leq$ 3.5 Å corresponds to "internal" trajectories; and the range $R >$ 3.5 Å corresponds to "external" trajectories passing outside the fullerene cage. The inset in Fig. 3,*b* shows fragments of the potential energy profiles at 2.1 Å $\leq R \leq$ 2.6 Å (magnified).

C(2)—H trajectory and corresponds to formation of the *exo*-H—C(2) bond.

Energy diagrams. As mentioned above, the potential energy profiles along the trajectories of the motion of the H atom were calculated assuming the same geometries of the fullerene cage. To obtain more correct energies and geometric parameters of the *endo*-H—C(2) and *exo*-H—C(2) bonds, we optimized the geometries of corresponding systems. Their energies calculated relative to the total energies of the $C_{59}X$ system and infinitely distant H atom (noninteracting reagents) are shown in Fig. 4. Encapsulation of the H atom at the center of the $C_{59}X$ sphere increases the energy of the H@$C_{59}X$ system by 28, 17, and 25 kcal mol^{-1} for X = B, N, and P, respectively. Displacement of the H atom from the center to the C(2) atom is followed by the formation of the *endo*-H—C(2) bond and the energy of the system decreases by 42 ($C_{59}B$), 27 ($C_{59}N$), and 41 ($C_{59}P$) kcal mol^{-1}. The major contribution to this decrease comes from the energies of the *endo*-H—C(2) bonds. The formation of the *exo*-H—C(2) bonds even more reduces the energy of the system, namely, by 80 ($C_{59}B$), 78 ($C_{59}N$), and 81 ($C_{59}P$) kcal mol^{-1}. The C—H(*exo*) bond energies approach the energies of ordinary C—H bonds (*cf.* ~80 kcal mol^{-1} in toluene). The C(2)—H(*endo*) and *exo*-H—C(2) bond lengths are listed in Table 3. In all molecules (for all X) the *exo*-bonds are shorter than the *endo*-bonds, which is consistent with the higher energies of the former. Noteworthy is an important feature, namely, the *exo*-H—C(2) bond energies

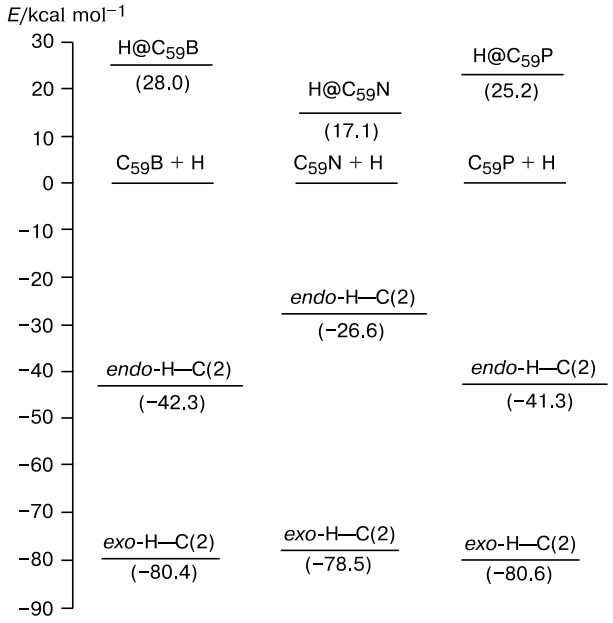

Fig. 4. Energies of differently organized systems H—$C_{59}X$ (X = B, N, P): noninteracting reagents $C_{59}X$ and H, endofullerenes H@$C_{59}X$, and heterofullerenes with the *exo*-H—C(2) and *endo*-H—C(2) bond. For notations, see text.

Table 3. H—C(2) bond lengths (*d*) in systems H—$C_{59}X$

X	*d*/Å	
	exo	*endo*
B	1.105	1.161
N	1.097	1.120
P	1.098	1.103

are almost equal for all X, whereas the energies of the *endo*-H—C(2) bonds are strongly different; they characterize the strain energy of the fullerene sphere, the strain being due to structural distortions upon formation of the *endo*-H—C(2) bond (see Fig. 4).

Thus, the $C_{59}X$ heterofullerenes can add an H atom to the C(2) atom to form a *endo*-H—C(2) and *exo*-H—C(2) bond. A common feature of all systems studied is that the energies of the *exo*-H—C(2) bonds are 40—50 kcal mol^{-1} higher than those of the corresponding *endo*-bonds. The energy difference between the *exo*- and *endo*-bonds characterizes different reactivities of the outer and inner surfaces of the fullerene sphere. The calculated spin densities and HFC constants on the X and ^{13}C atoms in the $C_{59}X$ radicals (X = B, N, P) made it possible to establish the pattern of the spin density distribution over the fullerene sphere.

The authors express their gratitude to B. N. Plakhutin for valuable comments and discussion of the results obtained.

This work was financially supported by the Council on Grants at the President of the Russian Federation (Program for State Support of Leading Scientific Schools in the Russian Federation, Grant NSh-5236-2006.3).

References

1. O. Vostrowsky and A. Hirsch, *Chem. Rev.*, 2006, **106**, 5191 (see also references cited therein).
2. J. C. Hummelen, B. Knight, J. Pavlovich, R. Gonzalez, and F. Wudl, *Science*, 1995, **269**, 1554.
3. C. Moschel and M. Jansen, *Z. Anorg. Allg. Chem.*, 1999, **625**, 175.
4. Y. Chai, V. Guo, C. Jin, R. E. Haufler, L. P. F. Chibante, J. Fue, L. Wang, J. M. Alford, and R. E. Smalley, *J. Phys. Chem.*, 1991, **95**, 7564.
5. R. R. Sahoo and A. Patnaik, *Chem. Phys. Lett.*, 2001, **394**, 201 (see also references cited therein).
6. A. L. Buchachenko and N. N. Breslavskaya, *Izv. Akad. Nauk. Ser. Khim.*, 2005, 51 [*Russ. Chem. Bull., Int. Ed.*, 2005, **54**, 51].
7. J. B. Foresman and E. Frish, *Exploring Chemistry with Electronic Structure Methods*, 2nd ed., Gaussian, Inc., Pittsburgh (PA), 1996, 302 pp.
8. M. J. Frisch, G. W. Trucks, H. B. Schlegel, G. E. Scuseria, M. A. Robb, J. R. Cheeseman, V. G. Zakrzewski, J. A.

Montgomery, Jr., R. E. Stratmann, J. C. Burant, S. Dapprich, J. M. Millam, A. D. Daniels, K. N. Kudin, M. C. Strain, O. Farkas, J. Tomasi, V. Barone, M. Cossi, R. Cammi, B. Mennucci, C. Pomelli, C. Adamo, S. Clifford, J. Ochterski, G. A. Petersson, P. Y. Ayala, Q. Cui, K. Morokuma, D. K. Malick, A. D. Rabuck, K. Raghavachari, J. B. Foresman, J. Cioslowski, J. V. Ortiz, A. G. Baboul, B. B. Stefanov, G. Liu, A. Liashenko, P. Piskorz, I. Komaromi, R. Gomperts, R. L. Martin, D. J. Fox, T. Keith, M. A. Al-Laham, C. Y. Peng, A. Nanayakkara, M. Challacombe, P. M. W. Gill, B. Johnson, W. Chen, M. W. Wong, J. L. Andres, C. Gonzalez, M. Head-Gordon, E. S. Replogle, and J. A. Pople, *GAUSSIAN-98,* Gaussian Inc., Pittsburgh (PA), 1998.

9. S. Stafström, L. Hulman, and N. Hellgren, *Chem. Phys. Lett.*, 2001, **340**, 227.
10. N. Kurita, K. Kobayashi, H. Kumamora, K. Tago, and K. Ozawa, *Chem. Phys. Lett.*, 1992, **198**, 95.
11. W. Andreoni, A. Curioni, K. Holczer, K. Prassides, M. Keshavarz-K., J.-C. Hummelen, and F. Wudl, *J. Am. Chem. Soc.*, 1996, **118**, 11335.
12. F. Fülöp, A. Rockenbauer, F. Simon, S. Pekker, L. Korecz, S. Garaj, and A. Jánossy, *Chem. Phys. Lett.*, 2001, **334**, 233.
13. J. Lu, Y. Zhou, Y. Luo, Y. Huang, X. Zhang, and X. Zhao, *Mol. Phys.*, 2001, **99**, 1203.
14. R. B. Darzynkiewicz and G. E. Scuseria, *J. Phys. Chem. A*, 1997, **101**, 7141.
15. J. M. Hawkins, A. Meyer, T. A. Lewis, S. D. Loren, and F. J. Hollander, *Science*, 1991, **252**, 312.
16. A. L. Buchachenko and A. M. Vasserman, *Stabil'nye radikaly* [*Stable Radicals*], Khimiya, Moscow, 1973, 408 pp. (in Russian).

Received December 25, 2006,
in revised form March 23, 2007